CHESS: Measuring the Dynamics of Composition and Density of Earth's Upper Atmosphere with CubeSats

Rico G. Fausch
University of Bern, Physics Institute
Sidlerstrasse 5
3012 Bern
rico.fausch@unibe.ch

Gregor Moeller
ETH Zürich, Institute of Geodesy and Photogrammetry
Robert-Gnehm-Weg 15, 8093 Zurich
gmoeller@ethz.ch

Markus Rothacher
ETH Zürich, Institute of Geodesy and Photogrammetry
Robert-Gnehm-Weg 15, 8093 Zurich
markus.rothacher@ethz.ch

Nicolas Martinod
Swiss Federal Institute of Technology in Lausanne (EPFL)
Rte Cantonale, 1015 Lausanne
nicolas.martinod@epfl.ch

Tristan Trébaol
Swiss Federal Institute of Technology in Lausanne (EPFL)
Rte Cantonale, 1015 Lausanne
tristan.trebaol @alumni.epfl.ch

Alfonso Villegas
Swiss Federal Institute of Technology in Lausanne (EPFL)
Rte Cantonale, 1015 Lausanne
alfonso.villegas@alumni.epfl.ch

Jean-Paul Kneib
Swiss Federal Institute of Technology in Lausanne (EPFL), School of Basic Sciences
Rte Cantonale, 1015 Lausanne
jean-paul.kneib@epfl.ch

François Corthay
University of Applied Sciences and Arts Western Switzerland Valais
Rue de l'Industrie 23
1950 Sion
francois.corthay@hevs.ch

Marcel Joss
Lucerne UAS, Inst. of Elect. Eng.
Technikumstrasse 21
6048 Horw
marcel.joss@hslu.ch

François Tièche
HE-Arc Engineering
Rue de la Serre 7
2610 St-Imier
francois.tieche@he-arc.ch

Marek Tulej
University of Bern, Physics Institute
Sidlerstrasse 5
3012 Bern
marek.tulej@unibe.ch

Peter Wurz
University of Bern, Physics Institute
Sidlerstrasse 5
3012 Bern
peter.wurz@unibe.ch

Abstract— **Earth's upper atmosphere is a dynamic system that is determined by external and internal forces. Understanding this system allows for insights into the evolution of a habitable world and, therefore, the origin of our Solar System. In addition, it is the environment for many satellites that are key to our modern world. The uppermost part of Earth's atmosphere, the exosphere and ionosphere, couples the collision-dominated thermosphere with outer space, where other processes determine the trajectories of the particles. Whereas the thermosphere is mostly gravitationally bound to the planet, a fraction of the particles present in the exosphere leaves Earth into interplanetary space. Over geologic times, these loss processes are an important factor in the evolution of an atmosphere and are considered being the main reason why Earth currently has a habitable atmospheric surface composition in contrast to Venus and Mars, which were all very similar once. In the short term, the variability of the Sun's radiation, including both photons (from XUV to IR) and energetic particles causes considerable variations in the chemical composition, the density, and the spatial extent of the exosphere. The exobase is located at about 300 km altitude and the exosphere extends to tens of thousands of kilometers. Detailed knowledge of the exosphere is not only interesting for our basic understanding but is also important for spacecraft in near-Earth orbits, like the International Space Station. Although density and chemical composition are closely related, our present knowledge depends on separate measurements of the chemical composition, performed in the early 1980s, and the density, mostly performed during the 1990s. To end this long data gap, the community requires new in-orbit composition measurements, and to overcome the time-space degeneracy, it is necessary to measure both the chemical composition and the density of the exosphere with a network of satellites at several locations simultaneously. The constellation of high-performance exospheric science satellites (CHESS) program comprises a constellation of two 3U CubeSats, and more units later, designed to create an inventory of chemical species present in the exosphere, measure the density, and record their variability over both space and time. Each satellite is equipped with a novel time-of-flight mass spectrometer for both density**

978-1-7281-7436-5/21/$31.00 ©2021 IEEE

measurements and highly sensitive chemical composition analysis of major to trace amounts of species. The payload is complemented by a new generation of dual-frequency global navigation satellite system (GNSS) receivers for precise orbit determination. It allows for computing the total density from estimates of atmospheric drag and the dispersive line-of-sight total electron content from the linear combination of dual-frequency carrier phase measurements. This pathfinder mission is the first step towards a permanent observation of the Earth's exosphere from several vantage points simultaneously. It is designed to provide scale heights of each chemical species, their altitude profiles and exospheric temperatures to determine atmospheric escape parameters. Furthermore, it allows for analyzing the spatial and temporal variability to infer the drivers of the exosphere including the impact of anthropogenic climate change, improve satellite orbital decay models, and test possibilities of capturing earthquake precursors.

TABLE OF CONTENTS

1. INTRODUCTION

Our detailed understanding of Earth's atmosphere becomes limited at the exobase. In the last decades, Earth's atmosphere has attracted considerable attention, especially regarding weather and climate change. Chemical composition, number density, and temperature influence these phenomena. Depending on the altitude and the measurement itself (for example, temperature, pressure, chemical composition such as humidity, ozone concentration, particulate matter pollution in cities, and more), there is a low latency between the actual measurement and the time of availability of the data. In fact, most Earth observation systems provide almost real-time data of measurements from the lower and middle atmosphere these days. This status contrasts the upper region of our atmosphere, which completely lacks real-time measurements or, even more recently published, reliable data of the chemical composition and exospheric temperature.

Measurements of the chemical composition of Earth's upper atmosphere led to the currently available models of the exosphere. Mass spectrometers analyzed species up to an upper mass limit of about *m/z* 50 [1]–[4] covering the mass range of the major species in the upper atmosphere (H, N, O, N_2, CO, NO, O_2, Ar; H^+, He^+, N^+, O^+, N_2^+). Measurements in this mass range were ceased after the successful measurements of the Dynamics Explorer launched in 1981 [4]. The resulting data provided updates to the Jacchia-70 type models using total mass density (inferred from orbital decay) [5] leading to the empirical (US) Naval Research Laboratory (NRL) – mass spectrometer and incoherent scatter radar models of the atmosphere (MSIS) MSIS-86 [6] and MSISE-90 [7]. COSPAR International Reference Atmosphere (CIRA) models have also been used, especially in climate modeling (see discussion in [8]) but were mostly replaced by the International Reference Ionosphere (IRI) model of the ionosphere [9]. NRLMSISE-00 [8] became the standard model for the chemical composition of species in the upper atmosphere for years. It was more recently upgraded with the NRLMSISE 2.0 [10] but both models still rely mostly on measurements of the lower thermosphere or mass spectrometric data of the 1980s. Although several groups have identified this gap, both missions and instruments designed to fill it either failed, or considerable vary in scientific performance, or are scheduled for launch in the (far) future [11]–[19]. However, the desire for updated data is persistent as illustrated by NASA science mission directorate's recent announcement on its planning for a Dynamical Neutral Atmosphere-Ionosphere Coupling (DYNAMIC) mission and the solicitation for the Geospace Dynamics Constellation (GDC) mission. Both missions will address the dynamics of the atmosphere.

Above about 200 km altitude, the atmosphere is strongly driven by electromagnetic forces resulting from the interaction of the solar wind with the Earth's magnetosphere. Thus, the dynamics in the upper atmosphere cannot solely be described by measurements of the neutral species but requires a profound understanding of the coupling processes between the thermosphere and ionosphere. Ionospheric models such as the latest release of the International Reference Ionosphere model (IRI-2016, [9]) can capture large parts of these dynamics but strongly depend on the synthesis of available and reliable measurements, for example, from ionosondes, incoherent scatter radars, rockets, topside sounders, and in-situ satellites. Further improvements in ionospheric modelling require a further densification of existing observing networks in critically under-sampled regions in the ionosphere, for example, in the form of global navigation satellite system (GNSS) based electron maps or topside profiles [9].

2. CONTEXT

The understanding of Earth's upper atmosphere directly connects to numerous research fields related to both basic research and applied science. This selection of topics provides insights into how society relies on this under-estimated dataset.

Earth's Upper Atmosphere

Earth's upper atmosphere is a complex region, as it has multiple drivers whose influences remain unclear. Depending on the usage, either the ionosphere or thermosphere-exosphere are considered. Parameters of interest are the chemical composition, number density, temperature, and total electron content. Whereas the ionosphere has significant amounts of ions and electrons, the thermosphere and exosphere mostly contain neutral species, as the abundance of the ions is about two decades lower. The thermosphere is characterized by the region in which many collisions of species statistically determine the particle trajectories and the macroscopic physical parameters (Knudson number $\ll 1$). The higher the altitude, the more the density decreases. Above the exobase, the particle trajectories of species are dominated by ballistic trajectories rather than by statistical collisions as observed in the thermosphere (Knudson number $\gg 1$). The transition from the thermospheric to the exospheric regions is the exobase that is estimated to be located at about 300 km altitude, where the Knudson number, i.e., the ratio of the mean free path to the characteristic length scale, is about 1. The Sun and other drivers influence the altitude of the exobase [20], [21]. Table 1 summarizes both drivers and driven processes as well as their characteristic timescale. Although all the drivers are thought to be identified (see e.g. [20], [22]–[24] and references), their exact influence remains largely unconstrained. Only new, highly sensitive and in situ measurements of the chemical composition, the number density, and the total electron content may advance this enduring debate.

Exospheres in Comparative Planetology

Exospheres represent the interface between interplanetary space and the celestial object. A fraction of the species present in the exosphere constantly leaves Earth into space. As the extent of these atmospheric escape processes is species dependent, atmospheres may evolve over their lifetime. A planet's atmosphere may evolve from a toxic atmosphere as found on present Venus to a life-bearing atmosphere as found on present Earth. Venus, Earth, and Mars are shown to have a very similar composition (rocky planets) and similar initial atmospheres during the times of the early Solar System [25]. Modeling the evolution of the Earth with these initial conditions and with the currently assumed atmospheric loss rates leads to a version of Earth that severely contradicts our today's observation, for example, a habitable planet [26]. As the difference in chemical composition of the atmospheres of three siblings cannot solely be explained by enhanced Jeans escape, a unique evolution of Earth has to be considered. In situ investigation of Mars' and Venus' atmospheres (Mars Express, Venus Express, and Mars Atmosphere and Volatile Evolution MAVEN) found a considerable non-thermal (ion) contribution to the atmospheric escape that could explain this inconsistency. However, no sufficiently accurate data of Earth's exosphere are available to conclude on this issue.

Currently, two methods exist to determine Earth's thermal escape: 1) Thermal escape can be modeled from the temperature and the density profiles of species by subtracting the superthermal contribution, which is inferred from velocity distributions of the species of present in the exosphere [27]. This approach requires a neutral and ion mass spectrometer for in situ measurements. 2) Plasma instruments are used to cover the complete energy range of ionic species to determine the energy distribution of them as well. The latter approach is currently not feasible given the size of the required instrumentation, especially for CubeSats.

Table 1. The time scales of selected phenomena indicate the possibility of the CHESS ability to analyze them.

Phenomena or driver	Typical timescale	CHESS-pathfinder	CHESS-live
Atmospheric escape	Constantly	YES	YES
Baseline for astrobiology	Constantly	YES	YES
Ionospheric disturbances	Minutes to days	YES	YES
Earthquake precursors	Hours to days	YES	YES
Night-side transport	1 day	YES	YES
Influence of the Moon	28 days	YES	YES
Total Electron Content (TEC) trends	Seasons to solar cycles	Partially	YES
Solar cycle	11 years	Partially	YES
Satellite drag models	25 years	Partially	YES
Climate change	Decades, but need start now	Partially	YES

Earth Observation, Space Weather, and Climate Change

Objects orbiting Earth as satellites constantly interact with energetic particles of the tenuous exosphere causing drag. Drag is beneficial as it causes space debris to decelerate and ultimately re-enter into Earth's atmosphere. Especially, CubeSat designers are encouraged to meet the Inter-Agency Space Debris Coordination Committee (IADC) orbit lifetime policy stating that objects shall re-enter 25 years upon end of life. The lifetime of satellites is modeled using the density (and chemical composition) of the exosphere, the geometry of the satellites, and orbital parameters. Forward propagation of orbital elements is already challenging in a short time scale, for example, for re-entry into Earth's atmosphere, but almost impossible in the requested lifespan as the density

models are poorly constrained. Another issue for satellite designers is the largely unknown chemical composition of the exosphere. On a microscopic scale, drag is caused by the constant bombardment of particles on a satellite's surface. This chemical sputtering degrades solar cells considerably, limiting their lifetime. Unfortunately, as the chemical composition has to be estimated and might be off by factors (e.g. [28]), designing appropriate surfaces remains an inefficient task.

The short-, medium-, and long-term dynamics of the upper atmosphere (human timescales) provide opportunities for humankind but may also involve threats. There is an ongoing discussion on the long-term trends and variations of the parameters defining the upper atmosphere as of anthropogenic origin [23], [29]–[33]. A cooling of the exosphere is shown, causing the exobase to contract to lower latitudes. The reduced drag at a given altitude implies an increased lifetime of objects in space. An increased lifetime of space debris may threaten both the access to space in the future and projects such as the international space station (ISS). In the medium-term, satellite operators depend on space weather forecasts. These forecasts are substantially complicated, as, among other reasons, not even the current status of the exosphere is exactly known. In short-term, possibilities to capture earthquake precursors have been suggested by identifying disturbances in the chemical composition and in the density (e.g. [34]–[37] and references). Further sophisticated, sensitive in situ measurements are needed to provide evidence for this hypothesis.

3. CHESS Mission Objectives

We conceived the constellation of high-performance exospheric science satellites (CHESS) mission to provide update data conducted with state-of-the-art, high-performance instrumentation. At a later stage, with more units, low latency of data collection will be realized. The CHESS mission will fill the gap of space-time degeneracy in chemical composition, number density measurements of the exosphere and electron density measurements of the ionosphere, with a network of satellites at several locations simultaneously. CHESS has three primary mission objectives:

A—Create an inventory of chemical species and determine the total electron content present in the exosphere and upper ionosphere to serve as a data archive for Earth observation including space weather and climate change, comparative planetology including astrobiology, and space mission design of satellites.

B—Analyze the temporal and spatial variability, for example, the dynamics, of the chemical composition of the species and the total electron content. To determine both the drivers themselves and their influence on the upper atmosphere in detail, we measure these variables each at an instance, locality (in the orbital plane) and along the line-of sight to the GNSS satellites in view. These measurements, separated both temporally and spatially, allow overcoming space-time degeneracy.

C—We use these data to couple them with data from other Earth observation services to establish a real-time monitoring system of Earth's upper atmosphere. The CHESS mission will determine the parameters of the follow-up mission, for example, constellation parameters such as number of needed satellites and orbit parameters, instruments on board the satellites, their parameters, and, especially, the need of further space-time-locking of the measurements.

4. Mission Concept

The CHESS program (Table 2) provides almost real-time data of the exosphere similar to other Earth observation satellites provide, for example, lower atmosphere weather data. The first mission of this program is the CHESS-pathfinder mission consisting of two satellites demonstrating the concept. Each satellite is equipped with a mass spectrometer and a GNSS instrument. In this paper, CHESS refers to the CHESS-pathfinder mission.

Table 2. Mission plan of the CHESS program. MS: Mass Spectrometer; GNSS: Global Navigation Satellite System; SSO: Sun-Synchronous Orbit; TBC: To Be Confirmed.

Mission	CHESS-pathfinder	CHESS-live
Satellites	2	> 8 (TBC)
Payload	MS, GNSS, Retroreflector	MS, GNSS, Retroreflectors and others
Orbital parameter	Elliptical 1,000 – 400 km apogee-perigee; SSO 550 km, 97.5° inclination	Elliptical and SSO (TBC)

The CHESS-pathfinder mission will determine the mission design of the follow-up mission CHESS-live. We investigate the necessity of adding additional payload such as, for example, plasma instruments, Lyman-alpha or ultraviolet instrument, energetic particle dosimeter, F10.7 antenna, and measure the chemical composition of negative ions, which are mostly present at lower altitudes. Moreover, the exact orbital parameters of CHESS-live will be assessed and improved if necessary.

Orbital Design and Measurement Concept

The initial constellation of CHESS consists of two satellites operating simultaneously to overcome time-space degeneracy. Figure 2 illustrates the measurement concept of CHESS. The first satellite is to be placed on a (circular) sun-synchronous orbit (SSO) at 550 km (~97.5° inclination). This orbit choice reflects that the Sun is considered as a major

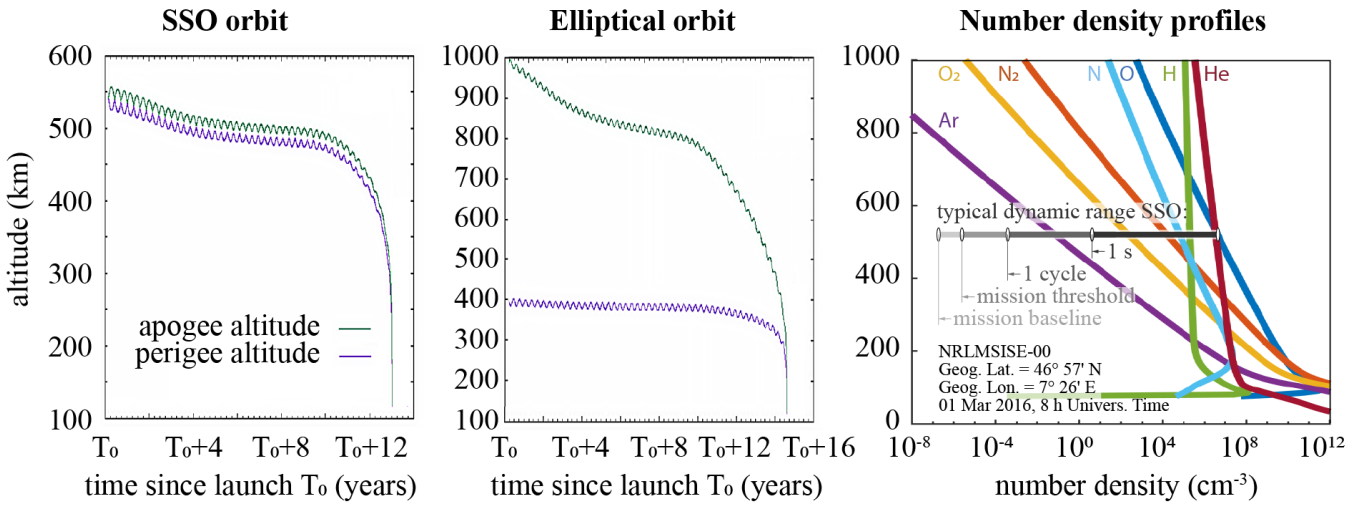

Figure 1. The altitude of the satellite in the circular orbit (left panel) and the elliptical orbit (central panel) decreases over time. Sample number density profiles are provided for reference including an anticipated dynamic range of the CubeSatTOF instrument in SSO (right panel). The simulation assumes T_0 to be late 2023.

driver for the variability of the exosphere. This satellite will make the measurements at a constant local time and altitude, hence, devoted for investigation of temporal effects such as diurnal cycle, night-side transport, and seasonal cycles. The second satellite is deployed on a coaxial elliptical orbital plane with 1000 – 400 km apogee–perigee. This satellite will establish altitude profiles of the exosphere's chemical composition and density, from which exospheric temperatures and atmospheric loss can be inferred.

The mission's lifetime is designed for a minimum of 2 years (baseline) to acquire a significant amount of data whilst meeting the 25 years IADC guidelines for space debris mitigation [38]. In fact, already two months of chemical composition data suffices to pass the threshold duration defined for the pathfinder mission. Graphs in Figure 1, left and center panel, show the flight trajectories of the two satellites modeled with ESA's Debris Risk Assessment and Mitigation Analysis (DRAMA) tool. For reference, a sample altitude profile of neutral species' number density is provided on the right panel, representing the best currently available knowledge ([39] inferred from [8]). The study foresees the launch T_0 for late 2023.

Once in orbit, the satellite's attitude is stabilized and scientific instruments are commissioned. A typical measurement campaign foresees measuring with both satellites simultaneously. On each satellite, both the mass spectrometer and GNSS instrument are operated simultaneously as well for several orbits to overcome space-time degeneracy and allow for a precise correlation of number density and chemical composition. Once the spacecraft's data buffer approaches its capacity, the scientific instruments are commanded to stand-by and the upcoming communication window is used to downlink the telemetry. For downlink, the spacecraft rotates to point its antennas towards the ground station. Depending on the availability of the ground station, up to two orbits are used for the downlink, allowing for recharging of the satellite's batteries. Upon downlink, the spacecraft receives telecommands likely initiating another measurement cycle.

Mission Operation Phase and the Solar Cycle

The solar cycle influences the trajectory of the spacecraft and their measurements because of the varying solar ultraviolet and particle environment during the cycle. Although determining the influence of this very issue is a study goal, we rely on data from the NRLMSIS 2.0 code [10]. In December 2019, the present solar cycle 25 started as defined by the last solar minimum. The solar maximum is expected to be reached in about 2025. During this phase, the solar irradiation increases. The heating causes the atmosphere to expand, the exobase will rise to higher altitudes, and particle escape might increase. For example, measurements of orbital drag data of objects in low earth orbit (LEO) indicated variations in number density of more than one decade at an altitude of 400 km during a solar cycle [20], [21]. This expansion is favorable as measurements closer to the exobase are desirable regarding models coupling the lower, middle, and upper atmosphere [10]. In principle, a highly elliptical orbit is favorable to measure altitude density profiles of

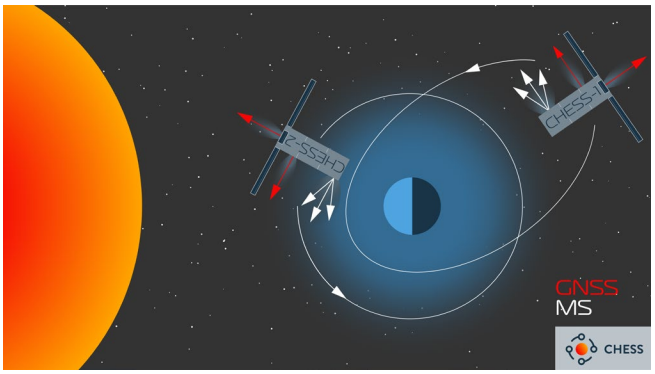

Figure 2. Schematic illustration of the measurement concept of the CHESS-pathfinder mission (orbits not to scale).

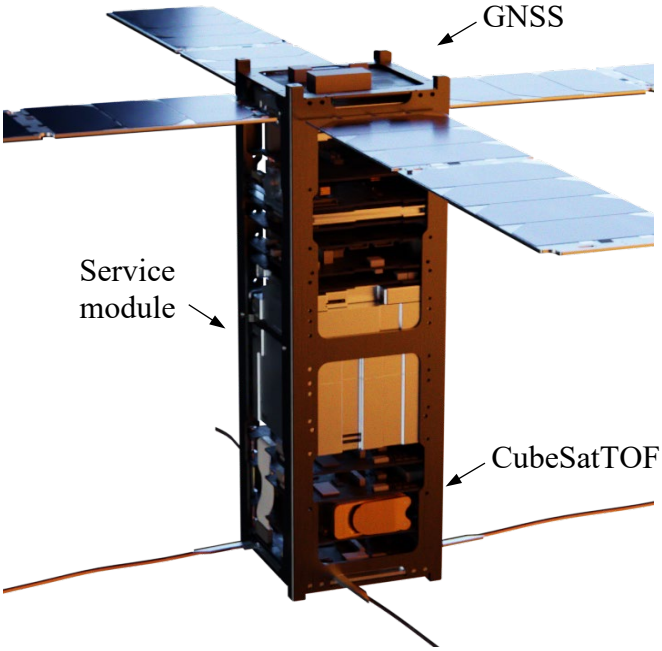

Figure 3. Computer aided design (CAD) model of the CHESS-1 satellite with the CubeSatTOF instrument (1 U, bottom), the satellite's service module (1.75 U, center), and the GNSS instrument (0.25 U, top), including two GNSS antennas on the zenith and rear facing side, respectively.

species over the complete mass range. However, approaching the exobase too close in such an orbit reduces the lifetime of the mission, thus, reducing the coverage of phenomena (stated in Table 1) that can be analyzed. To measure the phenomena over the longest possible time scales with the two satellites, we prioritized the lifetime of the satellite over the low altitude measurements at about 120 to 180 km [18]. A further advantage of this decision is that, during post-analysis, we have the possibility to histogram the recorded data to even increase the sensitivity of the mass spectrometer (see also Figure 1, right panel) [40].

The solar cycle and galactic cosmic ray (GCR) flux are anti-correlated. This relation positively influences the satellite's operating electronics given the reducing flux over the next years. Regarding the measurements themselves, the effect of GCRs will be investigated during post analysis. GCRs dominate the ionization of atmospheric particles below 70 km altitude (e.g. [41]).

CubeSat Platform

We minimize risks by relying on commercially available subsystems with flight heritage. A collaboration with a commercial provider of CubeSat platforms (Endurosat, Sofia, Bulgaria) is considered as baseline design. In this (evolved) scenario, they will supply their 3U platform. This platform includes a 42 Wh battery, with 60 W of peak power. The average energy available for the payloads equals 13 – 28 Wh per orbit (based on a 550 km SSO orbit). Four deployable solar panels provide power. An X-band transmitter will be used for payload downlink, with a configurable 1 – 30 Mbaud. For the telemetry and telecommands, an ultra high frequency (UHF) transceiver will be included. Figure 3 shows the service module and the compartments of the payloads.

Thermal Design

The thermal design foresees an active control of the temperature. The subsystem's common operational temperature ranges from 233 to 333 K (–40 to +60 °C), though, most of them have a specified minimum temperature of about 223 K (–50 °C). Figure 4 shows the expected global temperature profile of the satellite in SSO when operated in multiple configurations, for example, during measurements, stand-by, and downlink. One orbit corresponds to about 90 minutes. The presented analysis led to the conclusion that heaters need to be implemented as the lower limit of the temperature is reached for certain locations in the satellite.

Radiation Mitigation

Although LEO is considered as a moderate radiation environment, caution has to be taken if the corresponding orbital planes are inclined above about 55° latitude, given the increased flux of energetic particles from the terrestrial radiation belt. Therefore, the mission design was analyzed with the ESA's SPENVIS tool. To provide a reasonable probability of failure free operation over the baselined mission duration, a graded-Z composite of 1 mm Al – 0.1 mm Ta – 1 mm Al protects the electronics as it mitigates radiation effects of energetic particles, given the extensive use of commercial off-the-shelf (COTS) components. However, we decided using spot shielding, for example, with Ta or W, on selected components and subsystems depending on the last mass available. Although the exposure to the fluxes depends on the actual orbital parameters of a satellite, there is a strong tendency towards designing both satellites identically, which removes complexity from the systems engineering, rather than implementing more shielding on the exposed satellite (and less on the other) and make use of an average weight of both

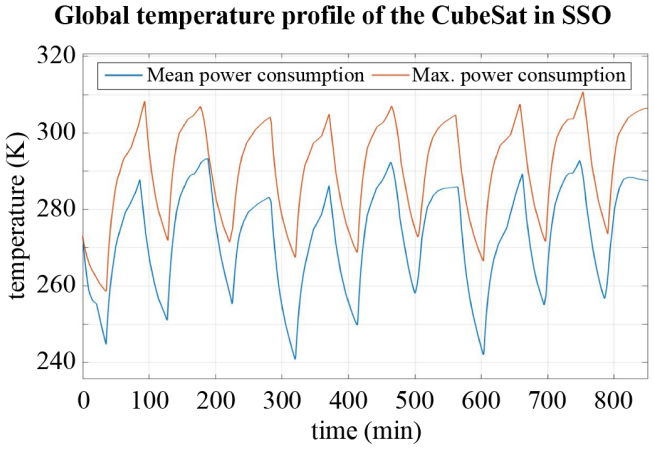

Figure 4. Modeled temperature profile of the CubeSat in the circular orbit.

satellites. In addition, although the payloads implement other radiation mitigation techniques as well, for example, selected high reliability (Hi-Rel) components, they further include shielding where suitable.

5. INSTRUMENTATION

Each CHESS satellite carries two major instruments: the mass spectrometer, CubeSatTOF, and the GNSS receivers. CubeSatTOF provides the chemical composition of both the neutral particles and ions and provides altitude profiles of number density data for each species, from which exospheric temperatures will be derived. These measurements are improved by GNSS receivers providing complementary data on the total electron content, which can be converted to the number density as well to improve the reliability of the data. In addition, the GNSS receivers provide a precise determination of each satellite's orbit, and the drag, from which estimates of atmospheric density can be derived.

The CubeSatTOF Instrument

The CubeSatTOF instrument is a neutral and ion mass spectrometer of 1U size for quantitative chemical composition analysis. It is described and characterized in detail in the references [39], [42]. This instrument uses the time-of-flight (TOF) technique to analyze species. TOF mass spectrometers have been widely used for the analysis of planetary atmospheres [43]–[46] since they measure the complete mass range simultaneously in about 100 ms translating at LEO to a spatial resolution of about 1 km, depending on orbit details.

Atmospheric processes include chemical reactions, the formation and destruction of molecular species. As we cannot observe the reactions themselves, we analyze the reactant and the product of such reactions statistically with a high sensitivity, allowing for identification of both major and minor processes. To do so, the CubeSatTOF instrument is designed to analyze species in a mass range *m/z* of about 1 to 200. The mass resolution which is necessary to achieve this mass range was recently demonstrated [39], [42].

The instrument features two options to distinguish between species originating from the spacecraft background and actual exosphere. The instrument provides a velocity dependent mass resolution providing selectivity by design [42]. When the CubeSatTOF instrument is operated in orbit mode (ion optical settings of the instrument), species enter the mass spectrometer with a defined velocity (for example, the spacecraft velocity). For analysis, they will be focused on the detector with nominal mass resolution and transmission. In contrast, slow, thermal species will have a lower mass resolution, allowing for a suppression of the gaseous background from the spacecraft. As of yet, the effect is more significant for higher masses, requiring the second option to be applied as well. This option foresees a rotation of the spacecraft, for example, during downlink, to point the CubeSatTOF's gas inlet opposite to the ram direction. By changing the configuration of the instrument to thermal gas mode, background measurements can be performed. The thermal gas mode analyzes the chemical composition of the ambient gas environment produced by constant outgassing of the spacecraft [47]. Figure 5 (after [39]) shows a typical mass spectrum acquired in thermal gas mode. During the subsequent data analysis, the separation between the signal from the atmosphere and the background of the spacecraft can be performed. Whereas comparable instruments reported on strict limitations concerning propellant [18], the CubeSatTOF instrument provides more flexibility, thanks to this background suppression. In addition, the proposed technique provides more reliability when interpreting the data.

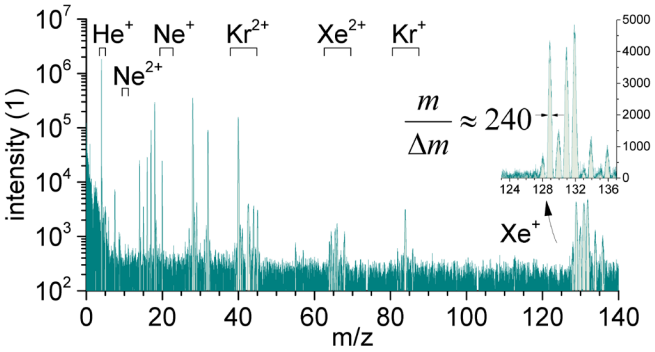

Figure 5. Typical mass spectrum of the CubeSatTOF instrument recorded in the laboratory with sample gas. The separated isotopes of xenon in the zoom indicate its mass range enabled by its mass resolution.

A further advantage of the CubeSatTOF instrument is that it measures the stream of gas incoming into the mass spectrometer directly. Thanks to this novel direct open source mass spectrometry technique (DOeS-MS), radicals and even heavy species preserve their chemical identity while entering the instrument. Thus, it can measure even complex (bio) molecules in its extended mass range. This allows for measurements of fragile, reactive and complex molecules such as O_3 and N_xO_y. A typical dynamic range of about 10^6 in 1 s can be reached by the CubeSatTOF instrument thanks to its heritage from the Neutral Gas Mass Spectrometer (NGMS) on board Luna-Resurs [44], [45], [48] and the Neutral and Ion Mass Spectrometer (NIM) on board the Jupiter Icy Moon Explorer (JUICE) [46]. A higher dynamic range can be achieved by accumulating the measurements during post processing [40] (see Figure 1, right panel) and by increasing the signal gain, which, however, clips the intense peaks. The provided dynamic range is sufficient to analyze the major and minor species in one cycle consisting of two orbits without clipping, which is the nominal use case. In addition, in dedicated measurement campaigns, the signal gain will be increased over several cycles to analyze even traces of species, thus, extending the dynamic range indicated in Figure 1, right panel. This is possible thanks to the sensitive read-out electronics. The electronics draw substantial heritage from the NGMS/Luna-Resurs design as well, but benefit from both COTS components (cheaper,

shorter lead time, part availability) and technological advancements. Basic concepts, including radiation mitigation techniques are described in [48].

The Dual-Frequency Multi-GNSS Receiver

For satellites in LEO, aerodynamic forces are acting on the surfaces of a satellite as of non-gravitational accelerations. These accelerations can be estimated together with the orbital parameters from GNSS measurements on board the satellite. Figure 6 shows the relation between GNSS position accuracy and temporal resolution, for example, how often atmospheric drag parameters can be estimated on board a LEO satellite at an altitude of 570 km.

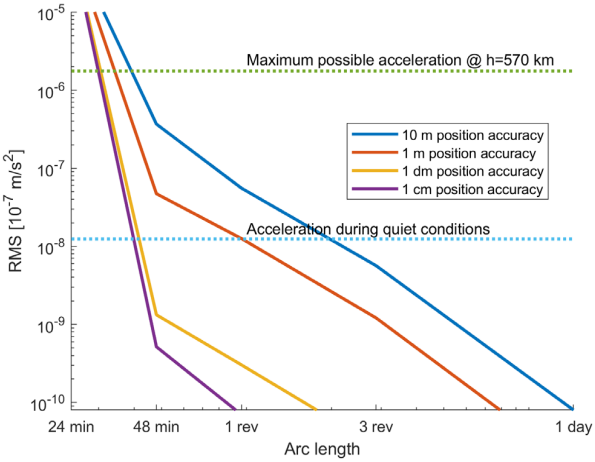

Figure 6. The impact of the GNSS position accuracy on the estimation of atmospheric drag parameters.

A GNSS position accuracy of 10 m allows for estimating the atmospheric density every 1 – 2 satellite revolutions. With cm to dm positioning, the temporal resolution improves by a multiple to about 30 minutes during quiet atmospheric conditions or even better during moderate conditions. To reach this high level of accuracy, one of the preconditions is that the GNSS receiver is dual-frequency. On the one hand, this allows for mitigating dispersive atmospheric effects; on the other hand, this also enables the study of these effects by estimating the total electron content (TEC) along the signal paths to more than a hundred of active GNSS satellites.

For the development of the GNSS payload board, in 2013 the Swiss Federal Institute of Technology Zürich (ETH) initiated the CubETH project with the vision to perform GNSS measurements with very efficient, small, low-cost and low-power GNSS receivers. The GNSS payload board selected for the CHESS mission is based on four u-blox ZED-F9P dual-frequency GNSS modules for centimeter level accuracy [49]. This power-efficient, low-weight GNSS receiver does not only allow for the tracking of all four GNSS on two frequencies with a sampling rate of up to 20 Hz, but also for the computation of real-time onboard solutions based on code and carrier phase measurements. Each of the four modules is connected to a zenith or rear facing GNSS patch antenna of the TAOGLAS GPSF.36.A series, respectively, for signal reception.

The core of the payload board will be an ARM Cortex (Arm Ltd.) microcontroller unit. Magnetoresistive random-access memory (MRAM) will be used for mission critical data, including configuration files and backup firmware images for the bootloader. The gathered scientific data will be stored on two redundant NOR-Flash memory partitions. All data will be equipped with appropriate checksums and stored redundantly, where applicable. To keep the costs at a reasonable level for this mission, all components of the payload board are selected as COTS components. The induced risk of COTS components is compensated by applying different measures to protect the board from radiation related effects. For example, with latch-up protection circuits and watchdogs and by adding enough redundancy to ensure that the mission survives a failure of certain components.

The GNSS payload features two main operation modes (Table 3) that provide the unique capability for continuous precise orbit determination (POD) and atmospheric profiling (ATM).

Table 3. GNSS main operation modes. GPS (G), GLONASS (R), Galileo (E), Beidou (C), Sampling rate of dual-frequency carrier phase measurements (Sampling), maximum data rate for download (Data rate) and maximum current consumption (Power).

Mode	GNSS	Sampling	Data rate	Power
POD	GREC	1.0 sec	2.5 kB/s	110 mA
ATM	G+E	0.1 sec	6.8 kB/s	170 mA

The resulting low-cost GNSS board fits into a 0.25 U form factor and, thus, is seen as the first step towards a permanent observation of the Earth's exosphere from several vantage points simultaneously. The modular design makes it a scalable and adaptable payload for the first two CHESS satellites, with some flexibility for follow-up missions.

For orbit validation, a retroreflector consisting of three corner cubes is mounted on the nadir-facing side of the satellite. This allows for the validation of the satellite orbit obtained from the GNSS measurements, and the air density values derived thereof, using the satellite laser ranging technique [50] with an accuracy of 1 – 2 cm.

6. Discussion

The presented CHESS mission allows for creating an inventory of chemical species and measuring the density of them to highest presently possible sensitivity on a 3 U CubeSat because of its modern instrumentation. These

measurements will provide long-needed, spatially and temporally correlated chemical composition and density data.

Earth's upper atmosphere is a dynamic system that is determined by external and internal forces causing phenomena in time scales ranging from seconds to the age of Earth. One of the key drivers of Earth's exosphere is the Sun. The Sun irradiates both photons (from extreme ultraviolet to infrared) and energetic particles. Despite Earth's magnetic field provides at least some shielding against particle radiation, the exosphere (and therefore the satellites orbiting in this region) is almost fully exposed to this irradiation. This irradiation penetrates towards the lower altitudes until it eventually reacts with an atmospheric particle. The result of this interaction causes various effects including atmospheric escape, ionization, and even single event effects potentially destroying electronics of satellites. The type of species that are ionized and the amount of ionization depend on the local time, with the ionized species together with the electrons forming the ionosphere of the Earth. In addition, Earth's rotation causes concentration gradients as the peak illumination moves over its surface. These effects cause night-side transport of species, which is poorly studied in Earth's exosphere. As the first CHESS satellite will be placed into a SSO to measure at locations of constant local times, we anticipate isolating the impact of the sun. In addition, we assume that other cyclic effects can be attributed (see also Table 1).

The different states and composition of the atmospheres of the three sibling planets Earth, Venus, and Mars are clearly observable today, but its different evolution remains unclear [51], [52]. By measuring the scale heights of each chemical species present in the exosphere and their altitude profile, global atmospheric escape rates, including exospheric temperatures, can easily be determined. The second satellite has an elliptical orbit to measure the altitude profile of the chemical species (and total electron content). Theoretical follow-up studies will use CHESS' data to indicate whether it is necessary to carry further plasma instrumentation to measure the ion escape at the same time. These data will provide knowledge for atmospheric escape processes, which is assumed the main reason for Earth having a habitable atmospheric surface composition, in contrast to Venus and Mars.

Although for most fields, for example, comparative planetology, short duration in situ measurements are already sufficient to push the frontier of science, applied research such as (space) weather prediction relies on continuous real-time data. For example, major earthquakes are thankfully seldom. The cumulative distribution of earthquakes is about proportional to 10^{-M} where M is the magnitude of the event (e.g. [53]). We assume that capturing precursors of such events is more likely the bigger their magnitude is, if feasible at all. Over the baseline (threshold) mission duration, the statistical global cumulative number of earthquakes exceeding magnitude 6.0 equals 134.1 (11.2), 31.4 (2.6) exceeding M 7.0, 1.5 (0.13) exceeding M 8.0, 0.08 (0.007) exceeding M 9.0, 0.02 (0.002) exceeding M 9.5, respectively [53], [54]. Despite the duty cycle for the downlink of the data, we expect to perform scientific measurements during M 7.0 events as part of the mission duration. Especially, the duty cycle, which is also needed for maintenance, indicates the need for a constellation of satellites. During the CHESS-pathfinder mission, sufficient data will be accrued to adapt the requirements of the successive CHESS-live satellites. The lessons learned from CHESS-pathfinder will help to establish a global monitoring system of Earth's exosphere.

7. SUMMARY

We presented a new mission, CHESS, to analyze the dynamics of the chemical composition and the number density of Earth's upper atmosphere with high-performance instrumentation. The CHESS-pathfinder mission will analyze the exosphere with two satellites in situ at the same time, each measuring with two instruments simultaneously to overcome space-time degeneracy. The mass spectrometer measures both major and minor components, and even traces of species, thanks to its acute sensitivity and mass range of about m/z 1 to 200. The GNSS instrument complements the mass spectrometer by measurements of the atmospheric density and total electron content. Empowered by this performance, these 3 U CubeSats can provide data to improve our knowledge of Earth's upper atmosphere with possible application in comparative planetology, satellite mission design, climate change, and Earth observation.

ACKNOWLEDGEMENTS

The authors represent a team working and studying at the HES Lucerne, HES-SO, EPFL, ETHZ, and University of Bern. We acknowledge all the unnamed contributors. EPFL and several of its associations funded both the development of the platform and the first tests of the satellite through founding the EPFL Spacecraft Team. The authors declare no conflict of interest.

REFERENCES

[1] D. T. Pelz, C. A. Reber, A. E. Hedin, and G. R. Carignan, "A neutral-atmosphere composition experiment for the Atmosphere Explorer-C, -D, and -E," *Radio Sci.*, vol. 8, no. 4, pp. 277–285, 1973, doi: 10.1029/RS008i004p00277.

[2] A. O. Nier, W. E. Potter, D. R. Hickman, and K. Mauersberger, "The open-source neutral-mass spectrometer on Atmosphere Explorer-C, -D, and -E," *Radio Sci.*, vol. 8, no. 4, pp. 271–276, Apr. 1973, doi: 10.1029/RS008i004p00271.

[3] A. E. Hedin, H. G. Mayr, C. A. Reber, G. R. Carignan, and N. W. Spencer, "A global empirical model of thermospheric composition based on OGO-6 mass spectrometer measurements," *Sp. Res.*, vol. 13, pp. 315–320, 1973.

[4] G. R. Carignan, B. P. Block, J. C. Maurer, A. E. Hedin, C. A. Reber, and N. W. Spencer, "The neutral mass spectrometer on Dynamics Explorer B," *Sp. Sci. Instrum.*, vol. 5, pp. 429–441, 1981.

[5] L. G. Jacchia, "New static models of the thermosphere and exosphere with empirical temperature profiles," *Smithson. Astrophys. Obs. Cambridge, Mass.*, 1970.

[6] A. E. Hedin, "MSIS-86 Thermospheric Model," *J. Geophys. Res.*, vol. 92, no. A5, p. 4649, 1987, doi: 10.1029/JA092iA05p04649.

[7] A. E. Hedin, "Extension of the MSIS Thermosphere Model into the middle and lower atmosphere," *J. Geophys. Res. Sp. Phys.*, vol. 96, no. A2, pp. 1159–1172, Feb. 1991, doi: 10.1029/90JA02125.

[8] J. M. Picone, A. E. Hedin, D. P. Drob, and A. C. Aikin, "NRLMSISE-00 empirical model of the atmosphere: Statistical comparisons and scientific issues," *J. Geophys. Res. Sp. Phys.*, vol. 107, no. A12, pp. 1–16, 2002, doi: 10.1029/2002JA009430.

[9] D. Bilitza, "IRI the International Standard for the Ionosphere," *Adv. Radio Sci.*, vol. 16, pp. 1–11, Sep. 2018, doi: 10.5194/ars-16-1-2018.

[10] J. T. Emmert *et al.*, "NRLMSIS 2.0: A Whole-Atmosphere Empirical Model of Temperature and Neutral Species Densities," *Earth Sp. Sci.*, vol. 8, no. 3, Mar. 2021, doi: 10.1029/2020EA001321.

[11] L. Kepko *et al.*, "Dellingr: NASA Goddard Space Flight Center's First 6U Spacecraft," in *Proceedings of the 31th Small Satellite Conference*, 2017, no. SSC17-III, pp. 1–12, [Online]. Available: https://digitalcommons.usu.edu/smallsat/2017/all2017/83/.

[12] M. Rodriguez *et al.*, "A Compact Ion and Neutral Mass Spectrometer for CubeSat/SmallSat Platforms," 2015, [Online]. Available: https://digitalcommons.usu.edu/smallsat/2015/all2015/103/.

[13] N. P. Paschalidis *et al.*, "Initial Results from the mini Ion and Neutral mass Spectrometer on the NSF Exocube and NASA Dellingr missions .," in *EPSC-DPS2019*, 2019, vol. 13.

[14] A. P. Agathanggelou *et al.*, "CIRCE: Coordinated Ionospheric Reconstruction Cubesat Experiment Alexander," in *Proceedings of the 34th Small Satellite Conference*, 2020, no. SSC20-III–02, pp. 1–7, [Online]. Available: https://digitalcommons.usu.edu/smallsat/2020/all2020/117/.

[15] G. D. R. Attrill *et al.*, "Coordinated Ionospheric Reconstruction CubeSat Experiment (CIRCE), In situ and Remote Ionospheric Sensing (IRIS) suite," *J. Sp. Weather Sp. Clim.*, vol. 11, p. 16, Feb. 2021, doi: 10.1051/swsc/2020066.

[16] J. W. Cutler, A. Ridley, and A. Nicholas, "Cubesat Investigating Atmospheric Density Response to Extreme Driving (CADRE)," in *Proceedings of the 25th Small Satellite Conference*, 2011, no. SSC11-IV–7, pp. 1–12.

[17] M. Guo *et al.*, "Performance evaluation of a miniature magnetic sector mass spectrometer onboard a satellite in space," *Eur. J. Mass Spectrom.*, vol. 24, no. 2, pp. 206–213, Apr. 2018, doi: 10.1177/1469066717741746.

[18] T. E. Sarris *et al.*, "Daedalus: a low-flying spacecraft for in situ exploration of the lower thermosphere–ionosphere," *Geosci. Instrumentation, Methods Data Syst.*, vol. 9, no. 1, pp. 153–191, Apr. 2020, doi: 10.5194/gi-9-153-2020.

[19] J. Klenzing *et al.*, "The petitSat mission – Science goals and instrumentation," *Adv. Sp. Res.*, vol. 66, no. 1, pp. 107–115, Jul. 2020, doi: 10.1016/j.asr.2019.12.013.

[20] J. T. Emmert, "A long-term data set of globally averaged thermospheric total mass density," *J. Geophys. Res. Sp. Phys.*, vol. 114, no. 6, pp. 1–17, 2009, doi: 10.1029/2009JA014102.

[21] J. T. Emmert, "Altitude and solar activity dependence of 1967-2005 thermospheric density trends derived from orbital drag," *J. Geophys. Res. Sp. Phys.*, vol. 120, no. 4, pp. 2940–2950, Apr. 2015, doi: 10.1002/2015JA021047.

[22] J. T. Emmert, "Thermospheric mass density: A review," *Adv. Sp. Res.*, vol. 56, no. 5, pp. 773–824, Sep. 2015, doi: 10.1016/j.asr.2015.05.038.

[23] J. Laštovička and Š. Jelínek, "A review of recent progress in trends in the upper atmosphere," *J. Atmos. Solar-Terrestrial Phys.*, vol. 163, no. March, pp. 2–13, Oct. 2017, doi: 10.1016/j.jastp.2017.03.009.

[24] G. W. Prölss, "Density Perturbations in the Upper Atmosphere Caused by the Dissipation of Solar Wind Energy," *Surv. Geophys.*, vol. 32, no. 2, pp. 101–195, 2011, doi: 10.1007/s10712-010-9104-0.

[25] E. Füri and B. Marty, "Nitrogen isotope variations in the Solar System," *Nat. Geosci.*, vol. 8, no. 7, pp. 515–522, Jul. 2015, doi: 10.1038/ngeo2451.

[26] H. Lammer *et al.*, "Constraining the early evolution of Venus and Earth through atmospheric Ar, Ne isotope and bulk K/U ratios," *Icarus*, vol. 339, no. November 2019, Mar. 2020, doi: 10.1016/j.icarus.2019.113551.

[27] R. T. Brinkmann, "Departures from jeans' escape rate for H and He in the earth's atmosphere," *Planet. Space Sci.*, vol. 18, no. 4, pp. 449–478, Apr. 1970, doi: 10.1016/0032-0633(70)90124-8.

[28] J. Krall, A. Glocer, M. C. Fok, S. M. Nossal, and J. D. Huba, "The Unknown Hydrogen Exosphere: Space Weather Implications," *Sp. Weather*, vol. 16, no. 3, pp. 205–215, 2018, doi: 10.1002/2017SW001780.

[29] S. C. Solomon, H. Liu, D. R. Marsh, J. M. McInerney, L. Qian, and F. M. Vitt, "Whole Atmosphere Simulation of Anthropogenic Climate Change," *Geophys. Res. Lett.*, vol. 45, no. 3, pp. 1567–1576, Feb. 2018, doi: 10.1002/2017GL076950.

[30] S. C. Solomon, H. L. Liu, D. R. Marsh, J. M. McInerney, L. Qian, and F. M. Vitt, "Whole Atmosphere Climate Change: Dependence on Solar Activity," *J. Geophys. Res. Sp. Phys.*, vol. 124, no. 5, pp. 3799–3809, 2019, doi: 10.1029/2019JA026678.

[31] A. D. Danilov and N. A. Berbeneva, "Some Applied Aspects of the Study of Trends in the Upper and Middle Atmosphere," *Geomagn. Aeron.*, vol. 61, no. 4, pp. 578–588, Jul. 2021, doi: 10.1134/S0016793221040046.

[32] J. Laštovička and Š. Jelínek, "Problems in calculating long-term trends in the upper atmosphere," *J. Atmos. Solar-Terrestrial Phys.*, vol. 189, no. October 2018, pp. 80–86, Aug. 2019, doi: 10.1016/j.jastp.2019.04.011.

[33] J. Laštovička, R. A. Akmaev, G. Beig, J. Bremer, and J. T. Emmert, "Global Change in the Upper Atmosphere," *Science*, vol. 314, no. 5803, pp. 1253–1254, Nov. 2006, doi: 10.1126/science.1135134.

[34] V. Korepanov, "Possibility to detect earthquake precursors using cubesats," *Acta Astronaut.*, vol. 128, pp. 203–209, Nov. 2016, doi: 10.1016/j.actaastro.2016.07.031.

[35] L. N. Doda, V. R. Dushin, V. L. Natyaganov, N. N. Smirnov, and I. V. Stepanov, "Earthquakes forecasts following space- and ground-based monitoring," *Acta Astronaut.*, vol. 69, no. 1–2, pp. 18–23, Jul. 2011, doi: 10.1016/j.actaastro.2011.02.012.

[36] T. V. Skorokhod and G. V. Lizunov, "Localized packets of acoustic gravity waves in the ionosphere," *Geomagn. Aeron.*, vol. 52, no. 1, pp. 88–93, Feb. 2012, doi: 10.1134/S0016793212010148.

[37] S. Jin, G. Occhipinti, and R. Jin, "GNSS ionospheric seismology: Recent observation evidences and characteristics," *Earth-Science Rev.*, vol. 147, pp. 54–64, 2015, doi: 10.1016/j.earscirev.2015.05.003.

[38] M. Yakovlev, "The 'IADC Space Debris Mitigation Guidelines' and supporting documents," in *4th European Conference on Space Debris*, 2005, vol. 587, pp. 591–597.

[39] R. Fausch, P. Wurz, U. Rohner, and M. Tulej, "CubeSatTOF: Planetary Atmospheres Analyzed with a 1U High-Performance Time-Of-Flight Mass Spectrometer," in *Proceedings of the 34th Small Satellite Conference*, 2020, no. SSC20-WKII-02, pp. 1–10, [Online]. Available: https://digitalcommons.usu.edu/smallsat/2020/all2020/14/.

[40] P. Wurz *et al.*, "Mass spectrometric analysis in planetary science: Investigation of the surface and the atmosphere," *Sol. Syst. Res.*, vol. 46, no. 6, pp. 408–422, Nov. 2012, doi: 10.1134/S003809461206007X.

[41] G. P. Brasseur and S. Solomon, *Aeronomy of the Middle Atmosphere*, vol. 32. Dordrecht: Springer Netherlands, 2005.

[42] R. G. Fausch, P. Wurz, B. Cotting, U. Rohner, and M. Tulej, "Direct Measurement of Neutral Gas during Hypervelocity Planetary Flybys," *2022 IEEE Aerosp. Conf.*, 2022.

[43] S. Scherer *et al.*, "A novel principle for an ion mirror design in time-of-flight mass spectrometry," *Int. J. Mass Spectrom.*, vol. 251, no. 1, pp. 73–81, Mar. 2006, doi: 10.1016/j.ijms.2006.01.025.

[44] D. Abplanalp *et al.*, "A neutral gas mass spectrometer to measure the chemical composition of the stratosphere," *Adv. Sp. Res.*, vol. 44, no. 7, pp. 870–878, Oct. 2009, doi: 10.1016/j.asr.2009.06.016.

[45] P. Wurz, D. Abplanalp, M. Tulej, and H. Lammer, "A neutral gas mass spectrometer for the investigation of lunar volatiles," *Planet. Space Sci.*, vol. 74, no. 1, pp. 264–269, 2012, doi: 10.1016/j.pss.2012.05.016.

[46] M. Föhn *et al.*, "Description of the Mass Spectrometer for the Jupiter Icy Moons Explorer Mission," in *2021 IEEE Aerospace Conference*, Mar. 2021, pp. 1–14, doi: 10.1109/AERO50100.2021.9438344.

[47] B. Schläppi *et al.*, "Influence of spacecraft outgassing on the exploration of tenuous atmospheres with in situ mass spectrometry," *J. Geophys. Res. Sp. Phys.*, vol. 115, no. A12313, Dec. 2010, doi: 10.1029/2010JA015734.

[48] R. G. Fausch *et al.*, "Flight electronics of GC-mass spectrometer for investigation of volatiles in the lunar regolith," *2018 IEEE Aerosp. Conf.*, pp. 1–13, 2018, doi: 10.1109/AERO.2018.8396788.

[49] u-blox, "ZED-F9P-02B Data sheet: u-blox F9 high precision GNSS module," 2021. Accessed: Oct. 01, 2021. [Online]. Available: https://www.u-blox.com/sites/default/files/ZED-F9P-02B_DataSheet_UBX-21023276.pdf.

[50] M. R. Pearlman, J. J. Degnan, and J. M. Bosworth, "The International Laser Ranging Service," *Adv. Sp. Res.*, vol. 30, no. 2, pp. 135–143, Jul. 2002, doi: 10.1016/S0273-1177(02)00277-6.

[51] M. Vázquez, E. Pallé, and P. M. Rodríguez, "The Earth in Time," in *The Earth as a Distant Planet: A Rosetta Stone for the Search of Earth-Like Worlds*, New York, NY: Springer New York, 2010, pp. 35–105.

[52] H. Lammer *et al.*, "Origin and evolution of the atmospheres of early Venus, Earth and Mars," *Astron. Astrophys. Rev.*, vol. 26, no. 1, pp. 1–72, 2018, doi: 10.1007/s00159-018-0108-y.

[53] F. Vallianatos, G. Michas, and G. Papadakis, "Nonextensive Statistical Seismology: An Overview," in *Complexity of Seismic Time Series*, Elsevier, 2018, pp. 25–59.

[54] R. McCaffrey, "Global frequency of magnitude 9 earthquakes," *Geology*, vol. 36, no. 3, p. 263, 2008, doi: 10.1130/G24402A.1.

BIOGRAPHY

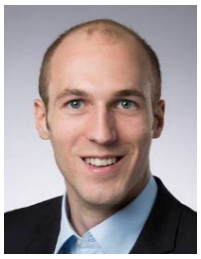

Rico G. Fausch *completed an apprenticeship as a mechanical design engineer before he received a B.Sc. in Systems Engineering (micro technologies) from NTB University of Applied Science (Switzerland) in 2013 and an M.Sc. in Biomedical Engineering from University of Bern (Switzerland) in 2015. He has been with the Physics Institute of the University of Bern since 2016, where he received his Ph.D. in Physics in 2020 for the finalization of the NGMS/Luna-Resurs. As a post-doctoral researcher, he is involved in the design of several space missions and space instrumentation including NIM/JUICE.*

Gregor Moeller *holds a Master's degree in Geodesy and Geophysics and a PhD in Technical Sciences from TU Vienna, Austria. In 2018, Gregor received a postdoctoral fellowship from NASA's Jet Propulsion Laboratory, where he was involved in the development of new CubeSat mission concepts for sensing the neutral atmosphere and ionosphere on Earth and Mars. Since Dec 2019, Gregor is a senior scientist in the group of Prof. Rothacher at ETH Zürich with a research focus on high-precision GNSS, atmospheric remote sensing, and orbit determination for dense CubeSat constellations.*

Markus Rothacher *received his PhD in Astronomy and his Habilitation in Space Geodesy from University of Berne. He was Professor for Space Geodesy at TU Munich from 1999-2004 and Professor for Geodetic Earth Sciences at TU Berlin from 2005 to 2009, being the Director of the Department "Geodesy and Remote Sensing" of the Deutsches GeoForschungsZentrum (GFZ) Potsdam. Since 2009 he is Professor for Mathematical and Physical Geodesy at ETH Zurich. His main research topic is high-precision GNSS. He was the PI of CHAMP and Co-PI of GRACE mission and is the Chair of the ESA Galileo Science Advisory Board (GSAC).*

Nicolas Martinod *will receive an M.Sc. in Robotics from the EPFL in 2022. In 2020, he co-founded the EPFL Spacecraft Team student association to support the development of the CHESS mission.*

Tristan Trébaol *received an M.Sc. in Mechanical Engineering from the EPFL in 2021. In 2020, he co-founded the EPFL Spacecraft Team student association to support the development of the CHESS mission.*

Alfonso Villegas *received an M.Sc. in Mechanical Engineering from the EPFL in 2021. He has worked with the EPFL Space Center as a Systems Engineer Intern from 2019. In 2020, he co-founded the EPFL Spacecraft Team student association to support the development of the CHESS mission.*

Jean-Paul Kneib *received the M.Sc. degree in astrophysics and space technology and the Ph.D. degree in astrophysics from Toulouse University, Toulouse, France, in 1990 and 1993, respectively. He worked as a Support Astronomer with European Southern Observatory (ESO), Munich, Germany. He has conducted research in gravitational lensing and cosmology in Cambridge, Toulouse, Caltech, and Marseille, before coming to the Swiss Federal Institute of Technology in Lausanne (EPFL), Lausanne, Switzerland. He is Director of the Laboratory of Astrophysics, and Director of the EPFL Space Center. He also leads the Swiss SKA Consortium.*

François Corthay *graduated at EPFL (Switzerland) in microtechnology in 1984. He received his Ph.D. in Science from Neuchâtel University (Switzerland) in 1992 for his work on oversampled digital filters. He presently teaches digital design at the University of Applied Sciences and Arts Western Switzerland Valais and participates to projects in the domain of digital control with programmable logic circuits. He has recently worked on the design of FPGA based On-Board Computers (OBC) for CubeSats.*

Marcel Joss *holds a degree in electrical engineering (HTL Windisch, 1986) and postgraduate degrees in system science (NTB Buchs, 1989), communication networks (EPFL, 1995) and international executive programme (INSEAD, 2000). Since 2005, he has been a professor at the Lucerne University of Applied Sciences and Arts, Institute of Electrical Engineering. He regularly gives lectures in communications engineering and microwave engineering. His research interests lie in the application area of microwave technology for communication systems, medical technology and industrial applications.*

François Tièche *has a B.Sc in Electronics (1981) and a M.Sc. in Computer Science from University of Neuchâtel (1990). He is professor at the University of Applied Sciences HE-Arc and was involved in the SwissCube project.*

Marek Tulej *received a Ph.D. in Physical Chemistry from the University of Basel in 1999. After his post-doctoral period at Paul Scherrer Institute, he joined in 2008 the University of Bern as an instrument scientist for space missions, including Phobos-Grunt, Marco Polo-R, Luna-Resurs, and JUICE.*

Peter Wurz *has a degree in electronic engineering (1985), an M.Sc. and a Ph.D. in Physics from Technical University of Vienna (1990). He has been a post-doctoral researcher at Argonne National Laboratory. At the University of Bern since 1992, he is a Professor of physics and since 2015 head of the Space Science and Planetology division. He has been Co-I and PI for many science instruments for space missions of ESA, NASA, ISRO, Roscosmos, and JAXA. He is PI of NIM and Co-PI of PEP on board JUICE.*